A Mindlin Shell Element That Satisfies Rigid-Body Requirements

J. S. Hansen* and G. R. Heppler†

University of Toronto, Ontario, Canada

Strain-displacement relations of the Mindlin type derived in shell coordinates for a general shell of arbitrary thickness and geometry are employed in the development of a finite element that can reproduce all rigid-body motions exactly. An approach to deriving basis functions which satisfies these requirements is presented and, as specific examples, basis functions for a circular cylinder, a circular cone, and a sphere segment are developed along with an exact means of numerical integration. The derived basis functions satisfy all completeness and compatibility requirements. The resulting finite element is compared to previous formulations in a number of different circular cylinder test cases and is shown to possess good accuracy and convergence properties.

Introduction

IN order to achieve monotonic convergence of a finite element formulation the trial functions should be complete and compatible. Completeness requires at least that the element be able to represent rigid-body displacements and constant strain states, while compatibility requires that the displacements within the element and across element boundaries be sufficiently continuous. Although it is well known that employing isoparametrically transformed elements to represent a shell geometry yields a formulation which automatically allows satisfaction of these requirements, there are instances where these approximate representations of the surface are unacceptable. For example, where nonlinear geometric effects are to be included and buckling is a potential problem, accurate geometric representation is important, since initial geometric imperfections have a drastic effect on buckling behavior. In the case of a general shell element formulated in shell coordinates, meeting the compatibility requirements is straightforward; however, satisfying the completeness requirements does pose difficulties.

With regard to completeness, the element must be capable of reproducing an incremental rigid-body motion without inducing a corresponding increment in strain energy. In a general shell element this means that it must be able to experience any combination of the six Cartesian translations and rotations without any strain occurring in the element. The ability of elements formulated in shell coordinates to reproduce a general rigid-body motion is a problem to which a good deal of interest[1-10] has been paid and a variety of solutions proposed. The basic problem encountered is that the relationship between displacements in shell coordinates and the rigid-body displacements involves trigonometric functions.[1-7] When the element displacement representation is given in terms of polynomials, it is impossible to reproduce all rigid-body modes exactly although they may be recovered for practical purposes in the limit as the element becomes very small. This results from the match of the Taylor series representation of the rigid-body motions and the corresponding trial functions. However, when a sufficient number of curved elements are employed to achieve this degree of approximation, it is often equally practical to employ flat facets to model the shell.[1]

Implicit addition of the rigid-body capability has been attempted for a four-node, thin, shallow circular cylinder element[1] and has produced an element formulation which is more complicated than would be found if pure polynomial trial functions were employed. The added complexity is offset by the fact that the resulting stiffness matrix has six zero eigenvalues as required for satisfaction of the general rigid-body motion requirements, and no nodal forces are introduced under a prescribed rigid-body motion. In the numerical examples presented the accuracy and convergence are quite good, but other applications of this element[10] show much poorer accuracy. Upon examining these trial functions it is found that the normal displacement "w" trial function neglects a number of low order terms and, thus, the trial functions are based on incomplete polynomials., For example, there is no constant term in the expression for the normal displacement and consequently a free-free cylinder subjected to a uniform pressure state cannot be modeled exactly. In addition, the trial function for the axial displacement "u" has effectively two constant terms which, in general, will not be independent.

Explicit addition of rigid-body motions to shell element stiffness matrices has been used[2,3,6,7] with interesting results. When the technique is applied to the circular cylinder element[2,6] that was modified implicitly in Ref. 1, the convergence rate for the pinch test problem increased and accuracy improved. Similarly, when the more general formulation[3,7] is applied to a circular cylinder good accuracy and convergence are exhibited in both the pinch and shell roof tests. However, when the explicit addition technique is applied to shells with double curvature (a sphere and a hyperboloid of revolution) the accuracy and convergence properties degenerated markedly compared to the cases where no rigid-body augmentation was used. The tests were: a sphere under uniform internal pressure, a spherical equivalent of the cylinder pinch test, and a hyperboloid cooling tower subjected to its own dead-weight loading. In all of these cases the results are very poor with rigid-body augmentation being applied and are excellent to fair without the augmentation. Fonder et al.[3,7] attribute this disparity of success between the cylinder cases and the general shell cases to the presence of nonzero Gaussian curvature in the sphere and hyperboloid geometries. It is also revealed that a posteriori addition of rigid-body modes renders the elements incompatible along the curved boundaries of an element. While in a practical sense the degree to which rigid-body motions must be represented depends on the problem under consideration, there are many problems where complete representation is essential.[11-13] Thus in the remainder of the paper the development of a finite element which satisfies all completeness and compatibility requirements will be outlined. This is followed by a discussion of results obtained with the present element and comparisons

Received Aug. 5, 1983; revision received March 15, 1984.

*Associate Professor, Institute for Aerospace Studies.

†Research Engineer, Institute for Aerospace Studies.

with other element formulations. The paper concludes with a summary of observations and conclusions.

Element Formulation

The use of Mindlin plate theory[14] in finite-element formulations for plates and shells is well established and has been shown to give good results[15-22] for moderately thick configurations. This approach has the advantage that independent displacement and rotation trial functions may be used and that these functions need only be C^0 continuous.

In order to treat moderately thick plates or shells it is necessary to include the transverse shear stresses τ_{yz} and τ_{zx} in the strain energy, while the normal stress σ_{zz} is considered to be negligible.[14] It has been shown[23-26] that, when the effect of transverse shear is included in a plate analysis, the normal deflection and rotation measure that is most convenient to use is a weighted average of the normal deflection over the thickness of the plate and a pair of rotation variables that are "equivalent to but not identical with the components of the change of slope of the normal to the undeformed middle surface."[23] This is because it is necessary to allow the normal displacement and rotations to vary through the thickness when transverse shears are present[23-27] and the weighted average interpretation allows this dependence to be included implicitly. With this in mind, the displacements are represented in the form

$$u=\bar{u}(x,y)+z\psi_x(x,y) \tag{1}$$

$$v=\bar{v}(x,y)+z\psi_y(x,y) \tag{2}$$

$$w=\bar{w}(x,y) \tag{3}$$

where for $\bar{u}$ and $\bar{v}$ the overbar indicates a displacement at the midsurface and, as indicated above, $\bar{w}$, ψ_x, and ψ_y are the measures of normal displacement and rotation.

The element is formulated for the analysis of plates and shells of small to medium thickness and is based on the use of shell coordinates. Thus, an accurate geometric representation is achieved which overcomes the difficulties that approximations to the geometry can produce.[28] Correspondingly, the following linearized strain-displacement relations will be utilized.[29,30]

$$\epsilon_{xx}=\frac{1}{\alpha}\left[\frac{\partial u}{\partial x}+\frac{v}{\beta}\frac{\partial \alpha}{\partial y}+w\frac{\partial \alpha}{\partial z}\right] \tag{4}$$

$$\epsilon_{yy}=\frac{1}{\beta}\left[\frac{\partial v}{\partial y}+\frac{u}{\alpha}\frac{\partial \beta}{\partial x}+w\frac{\partial \beta}{\partial z}\right] \tag{5}$$

$$\gamma_{xy}=\frac{1}{\beta}\frac{\partial u}{\partial y}+\frac{1}{\alpha}\frac{\partial v}{\partial x}-\frac{v}{\alpha\beta}\frac{\partial \beta}{\partial x}-\frac{u}{\alpha\beta}\frac{\partial \alpha}{\partial y} \tag{6}$$

$$\gamma_{yz}=\frac{\partial v}{\partial z}+\frac{1}{\beta}\frac{\partial w}{\partial y}-\frac{v}{\beta}\frac{\partial \beta}{\partial z} \tag{7}$$

$$\gamma_{zx}=\frac{\partial u}{\partial z}+\frac{1}{\alpha}\frac{\partial w}{\partial x}-\frac{u}{\alpha}\frac{\partial \alpha}{\partial z} \tag{8}$$

where (x,y,z) are orthogonal curvilinear coordinates on the surface of the shell u,v the tangential displacements in the x and y directions, respectively, w the normal displacement, and α and β are the Lamé coefficients.

In order that the present results not be restricted to thin, shallow shells, the factors $1/\alpha$ and $1/\beta$ are expanded in binomial series truncated to terms of $\mathcal{O}(z^2)$. The strain-displacement relations then take the form[31]

$$\epsilon=[B_0+zB_1+z^2B_2]=\sum_{i=0}^{2}B_iz^id \tag{9}$$

where $d=[\bar{u},\ \bar{v},\ \bar{w},\ \psi_x,\ \psi_y]^T$.

For the present formulation, the stress-strain relation corresponding to a linear-elastic, homogeneous, isotropic material is given by $\sigma=[D]\epsilon$ where the constitutive relation $[D]$ is derived from the general three-dimensional relation by assuming $\sigma_{zz}=0$ and contains corrections to the transverse shear terms as described by Mindlin.[14]

Incorporating the strain-displacment and constitutive relations in the strain energy functional yields

$$U=\frac{1}{2}\int_v d^T\left[\sum_{i=0}^{2}B_iz^i\right]^T[D]\left[\sum_{j=0}^{2}B_jz^j\right]d\mathrm{d}V \tag{10}$$

where, for a general shell, $\mathrm{d}V=\alpha\beta\mathrm{d}x\mathrm{d}y\mathrm{d}z$.

The displacments $\bar{u}$, $\bar{v}$, $\bar{w}$, ψ_x, and ψ_y are represented in the usual manner by employing a suitable set of basis functions N_i such that

$$\zeta=\sum_{i=1}^{m}N_i\zeta_i \tag{11}$$

where ζ is some general shell degree of freedom. When evaluating the stiffness matrix derived from Eq. (10), exact integration through the thickness is utilized where the terms of $\mathcal{O}(z^3)$ and greater in the integrand are neglected.

Basis Functions

As mentioned earlier, the trial functions are required to satisfy the rigid-body motion requirements of the shell element. The kinematic relations between the shell coordinate degrees of freedom and the six possible rigid-body degrees of freedom, referenced to some convenient Cartesian frame, in general can be expressed by

$$d=T(x,y)\delta \tag{12}$$

where d is the vector of shell displacements, in this case ($\bar{u}$, $\bar{v}$, $\bar{w}$, ψ_x, ψ_y), and δ is the vector of rigid-body translations and rotations. The three rigid-body translations are designed by (δ_x, δ_y, δ_z) and are parallel to the X, Y, and Z axes of the reference Cartesian frame, respectively. The three rotations are about the X, Y, and Z axes and are represented by (θ_x, θ_y, θ_z). The transformation T is generally a function of the shell coordinates (x, y).

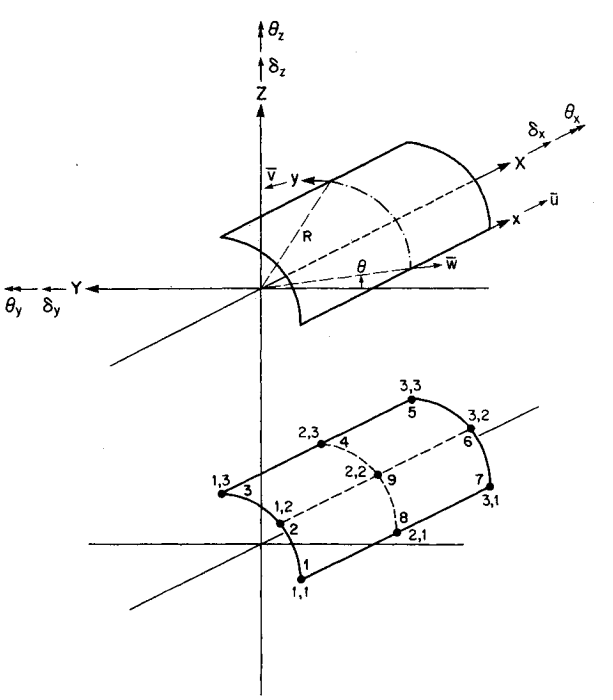

Fig. 1 Circular cylinder shell segment and implicit rigid-body element.

Again considering some general shell degree of freedom, ζ, it is assumed that the trial function may be cast in the form

$$\zeta = \sum_{i=1}^{m} \sum_{j=1}^{n} \zeta_{ij} G_i(\xi) H_j(\eta) \tag{13}$$

where ζ_{ij} is the value of ζ at the ijth of $m \times n$ nodes and $G_i(\xi)$, $H_j(\eta)$ are basis functions which are to be determined. In doing so, attention is being restricted to rectangular elements where curvilinear coordinates (ξ, η) coincide with lines of principal curvature. The intent is that $G_i(\xi)$, $H_j(\eta)$ will be basis functions of a form analogous to the form Lagrangian basis functions take.

The kinematic relationship (12) will act as a constraint on the form that the basis functions will take. That is, in order to determine the minimum requirement for $G_i(\xi)$, $H_j(\eta)$ it is imposed that these functions must be capable of reproducing rigid-body motions exactly when required to do so. Then the form of $G_i(\xi)$ may be determined by substituting Eq. (13) into Eq. (12) and setting $\eta = \eta_0 = \text{const}$ and the form of $H_j(\eta)$ may be determined by setting $\xi = \xi_0 = \text{const}$. The procedure will now be demonstrated for the case of a circular cylindrical shell.

Consider the shell segment illustrated in Fig. 1 which exhibits six rigid-body degrees of freedom. The kinematic relationship between the rigid-body degrees of freedom and the shell degrees of freedom is given by

$$\begin{bmatrix} \bar{u} \\ \bar{v} \\ \bar{w} \\ \psi_x \\ \psi_y \end{bmatrix} = \begin{bmatrix} 1 & 0 & 0 & 0 & R\sin\theta & R\cos\theta \\ 0 & \sin\theta & \cos\theta & -R & x\cos\theta & x\sin\theta \\ 0 & -\cos\theta & \sin\theta & 0 & -x\sin\theta & x\cos\theta \\ 0 & 0 & 0 & 0 & \sin\theta & \cos\theta \\ 0 & 0 & 0 & -1 & 0 & 0 \end{bmatrix} \begin{bmatrix} \delta_x \\ \delta_y \\ \delta_z \\ \theta_x \\ \theta_y \\ \theta_z \end{bmatrix} \tag{14}$$

Since (x, θ) are orthogonal coordinates, these may be considered to take the roles of (ξ, η) in Eq. (13). It is noted that a trial function corresponding to a 3×3 network of nodes has been taken for each element. This represents the minimum requirement for $H_j(\theta)$ (as will be seen) and a similar choice has been made in the x coordinate for purposes of symmetry. Employing the trial function form for $\bar{u}$ [Eq. (13)] in Eq. (14) yields

$$\sum_{i=1}^{3} \sum_{j=1}^{3} \bar{u}_{ij} G_i(x) H_j(\theta) = \delta_x + R(\sin\theta)\theta_y + R(\cos\theta)\theta_x \tag{15}$$

Now at the nodal points along an $x = x_1 = \text{const}$ meridian

$$\begin{aligned} \bar{u}_{11} &= \delta_x + RS_1\theta_y + RC_1\theta_x \\ \bar{u}_{12} &= \delta_x + RS_2\theta_y + RC_2\theta_x \\ \bar{u}_{13} &= \delta_x + RS_3\theta_y + RC_3\theta_x \end{aligned} \tag{16}$$

and similarly for $\bar{u}_{21}$, $\bar{u}_{22}$, $\bar{u}_{23}$ corresponding to $x = x_2$ and $\bar{u}_{31}$, $\bar{u}_{32}$, $\bar{u}_{33}$ corresponding to $x = x_3$ where S_j, C_j are sine and cosine evaluated at a node corresponding to θ_j. Substituting for $\bar{u}_{11}$, $\bar{u}_{12}$, $\bar{u}_{13}$ from Eq. (16) into Eq. (15), and then equating the coefficient of δ_x, θ_x, θ_y to zero yields

$$\begin{bmatrix} 1 & 1 & 1 \\ S_1 & S_2 & S_3 \\ C_1 & C_2 & C_3 \end{bmatrix} \begin{bmatrix} H_1^R \\ H_2^R \\ H_3^R \end{bmatrix} = \begin{bmatrix} 1 \\ \sin\theta \\ \cos\theta \end{bmatrix} \tag{17}$$

From this expression it follows immediately that the simplest basis functions which satisfy rigid-body motion requirements H_1^R, H_2^R, H_3^R must be functions of 1, $\sin\theta$, $\cos\theta$ and this functional dependence can be determined by inverting the matrix on the left-hand side of Eq. (17). Doing so yields

$$\begin{aligned} H_1^R(\theta) &= \frac{(S_\theta - S_2)(C_2 - C_3) - (C_\theta - C_2)(S_2 - S_3)}{(S_1 - S_2)(C_2 - C_3) - (C_1 - C_2)(S_2 - S_3)} \\ H_2^R(\theta) &= \frac{(S_\theta - S_3)(C_3 - C_1) - (C_\theta - C_3)(S_3 - S_1)}{(S_2 - S_3)(C_3 - C_1) - (C_2 - C_3)(S_3 - S_1)} \\ H_3^R(\theta) &= \frac{(S_\theta - S_1)(C_1 - C_2) - (C_\theta - C_1)(S_1 - S_2)}{(S_3 - S_1)(C_1 - C_2) - (C_3 - C_1)(S_1 - S_2)} \end{aligned} \tag{18a}$$

which are more concisely expressed as

$$\begin{aligned} H_1^R(\theta) &= \frac{\sin(\theta - \theta_2) - \sin(\theta - \theta_3) + \sin(\theta_2 - \theta_3)}{\sin(\theta_1 - \theta_2) - \sin(\theta_1 - \theta_3) + \sin(\theta_2 - \theta_3)} \\ H_2^R(\theta) &= \frac{\sin(\theta - \theta_3) - \sin(\theta - \theta_1) + \sin(\theta_3 - \theta_1)}{\sin(\theta_2 - \theta_3) - \sin(\theta_2 - \theta_1) + \sin(\theta_3 - \theta_1)} \\ H_3^R(\theta) &= \frac{\sin(\theta - \theta_1) - \sin(\theta - \theta_2) + \sin(\theta_1 - \theta_2)}{\sin(\theta_3 - \theta_1) - \sin(\theta_3 - \theta_2) + \sin(\theta_1 - \theta_2)} \end{aligned} \tag{18b}$$

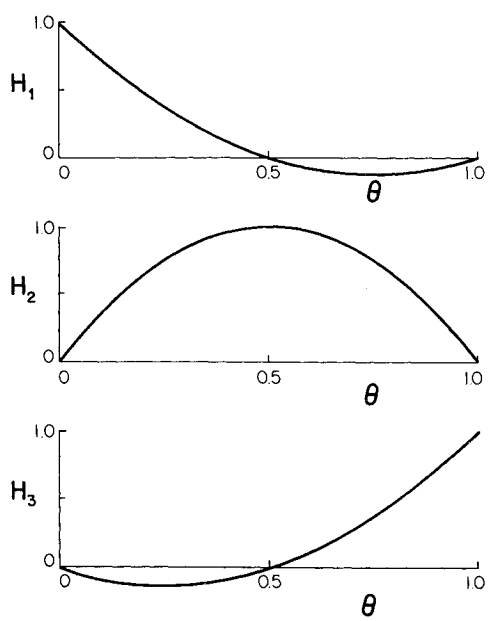

Fig. 2 Trigonometric basis functions.

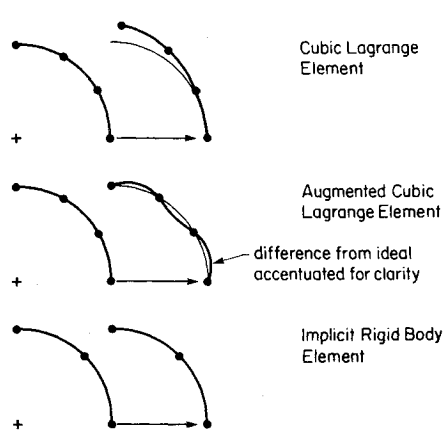

Fig. 3 Prescribed translation results.

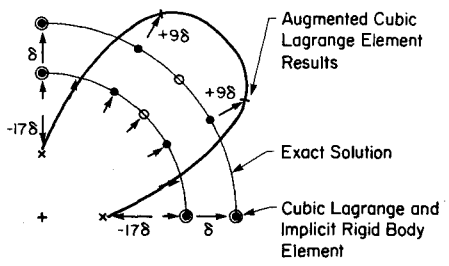

Fig. 4 Uniform pressure test results.

These functions have the general characteristics of finite element polynomial-based trial functions in that they have value unity at the node to which the trial function corresponds and value zero at all other nodes. It is also noted that these same basis functions could have been developed by observing that the right-hand side of Eq. (17) is dependent only on (1, $\sin\theta$, $\cos\theta$) and, thus, $H_i^R(\theta)$ need depend only on these functions.

Proceeding in a similar manner for $\bar{v}$, $\bar{w}$, ψ_x, ψ_y produces identical results for $\bar{v}$ while $H_j^R(\theta)$ corresponding to $\bar{w}$, ψ_x need only be functions of $\sin\theta$, $\cos\theta$, while those corresponding to ψ_y need only be constant. Thus the simplest choice for $H_j(\theta)$, which is valid for all degrees of freedom, corresponds to that of Eq. (18) with

$$H_j(\theta) \equiv H_j^R(\theta) \tag{19}$$

These basis functions are plotted in Fig. 2. Although the curves obtained from these basis functions are different from those which would be obtained from a set of Lagrangian quadratic basis functions over the same interval, the difference is so small as to be indiscernible in these figures.

The extension to elements for a higher number of nodes in the circumferential direction which are required to be functions of (1, $\sin\theta$, $\cos\theta$) follows readily and requires an odd number of nodes greater than three, that is, 5, 7, 9,..., corresponding to the basic functional forms involving (1, $\sin\theta$, $\cos\theta$, $\sin2\theta$, $\cos2\theta$), etc. The second-order (denoted by the superscript 2) trial functions for a five-node case are:

$$H_1^2 = \frac{[\sin(\theta-\theta_2)-\sin(\theta-\theta_3)+\sin(\theta_2-\theta_3)][\sin(\theta-\theta_4)-\sin(\theta-\theta_5)+\sin(\theta_4-\theta_5)]}{[\sin(\theta_1-\theta_2)-\sin(\theta_1-\theta_3)+\sin(\theta_2-\theta_3)][\sin(\theta_1-\theta_4)-\sin(\theta_1-\theta_5)+\sin(\theta_4-\theta_5)]}$$

$$H_2^2 = \frac{[\sin(\theta-\theta_3)-\sin(\theta-\theta_4)+\sin(\theta_3-\theta_4)][\sin(\theta-\theta_5)-\sin(\theta-\theta_1)+\sin(\theta_5-\theta_1)]}{[\sin(\theta_2-\theta_3)-\sin(\theta_2-\theta_4)+\sin(\theta_3-\theta_4)][\sin(\theta_2-\theta_5)-\sin(\theta_2-\theta_1)+\sin(\theta_5-\theta_1)]}$$

$$H_3^2 = \frac{[\sin(\theta-\theta_4)-\sin(\theta-\theta_5)+\sin(\theta_4-\theta_5)][\sin(\theta-\theta_1)-\sin(\theta-\theta_2)+\sin(\theta_1-\theta_2)]}{[\sin(\theta_3-\theta_4)-\sin(\theta_3-\theta_5)+\sin(\theta_4-\theta_5)][\sin(\theta_3-\theta_1)-\sin(\theta_3-\theta_2)+\sin(\theta_1-\theta_2)]}$$

$$H_4^2 = \frac{[\sin(\theta-\theta_5)-\sin(\theta-\theta_1)+\sin(\theta_5-\theta_1)][\sin(\theta-\theta_2)-\sin(\theta-\theta_3)+\sin(\theta_2-\theta_3)]}{[\sin(\theta_4-\theta_5)-\sin(\theta_4-\theta_1)+\sin(\theta_5-\theta_1)][\sin(\theta_4-\theta_2)-\sin(\theta_4-\theta_3)+\sin(\theta_2-\theta_3)]}$$

$$H_5^2 = \frac{[\sin(\theta-\theta_1)-\sin(\theta-\theta_2)+\sin(\theta_1-\theta_2)][\sin(\theta-\theta_3)-\sin(\theta-\theta_4)+\sin(\theta_3-\theta_4)]}{[\sin(\theta_5-\theta_1)-\sin(\theta_5-\theta_2)+\sin(\theta_1-\theta_2)][\sin(\theta_5-\theta_3)-\sin(\theta_5-\theta_4)+\sin(\theta_3-\theta_4)]} \tag{20}$$

The ease with which these basis functions may be extended to higher order is evident.

If the same avenue of approach is taken for constant θ generators, it is found that $G_i(x)$ need only be linear and, thus, it is more than adequate to adopt quadratic Lagrange polynomials as the basis functions. Denoting these by $G_i(x) \equiv L_i(x)$, the basis functions for the circular cylinder shell element, shown in Fig. 1, are

$$N_1 = L_1(x)H_1(\theta); \quad N_2 = L_1(x)H_2(\theta); \quad N_3 = L_1(x)H_3(\theta)$$

$$N_4 = L_2(x)H_3(\theta); \quad N_5 = L_3(x)H_3(\theta); \quad N_6 = L_3(x)H_2(\theta)$$

$$N_7 = L_3(x)H_1(\theta); \quad N_8 = L_2(x)H_1(\theta); \quad N_9 = L_2(x)H_2(\theta) \tag{21}$$

Here it should be noted that these basis functions also satisfy the rigid-body motion requirements of a conical shell segment as given by Dawe[4] and by replacing $L_i(x)$ by $H_i(x)$, with a suitable redefinition of x, the resulting basis functions will satisfy the rigid-body requirements of a segment of a sphere. Also, this approach to deriving basis functions may be used for other shell configurations which may be arithmetically more difficult to treat than the example given here but not conceptually more difficult. Furthermore, they satisfy the requirements of completeness by implicitly allowing strain-free rigid-body motions and they can reproduce constant strain states. There is continuity of the element degrees of freedom across element boundaries thus satisfying the conforming or compatibility condition.[32]

Numerical Integration

Three-point Gaussian quadrature will be able to integrate the Lagrangian function portion of the strain energy exactly; however, using any order of Gaussian quadrature on the trigonometric basis functions effectively replaces the trigonometric functions, which are essential to the rigid-body motion capability, with polynomials. Consequently, the rigid-body representation would be destroyed if Gaussian quadrature were used. The problem is easily resolved.

In the strain energy expression there will be functions of the form

$$\Gamma(\theta) = C_0 + C_1\sin\theta + C_2\cos\theta + C_3\sin^2\theta + C_4\sin\theta\cos\theta + C_5\cos^2\theta \tag{22}$$

which may be expressed as

$$\Gamma(\theta) = d_0 + d_1\sin\theta + d_2\cos\theta + d_3\sin2\theta + d_4\cos2\theta \tag{23}$$

with suitable definitions for d_i, $i=0, 4$ ($M=4$). Note that

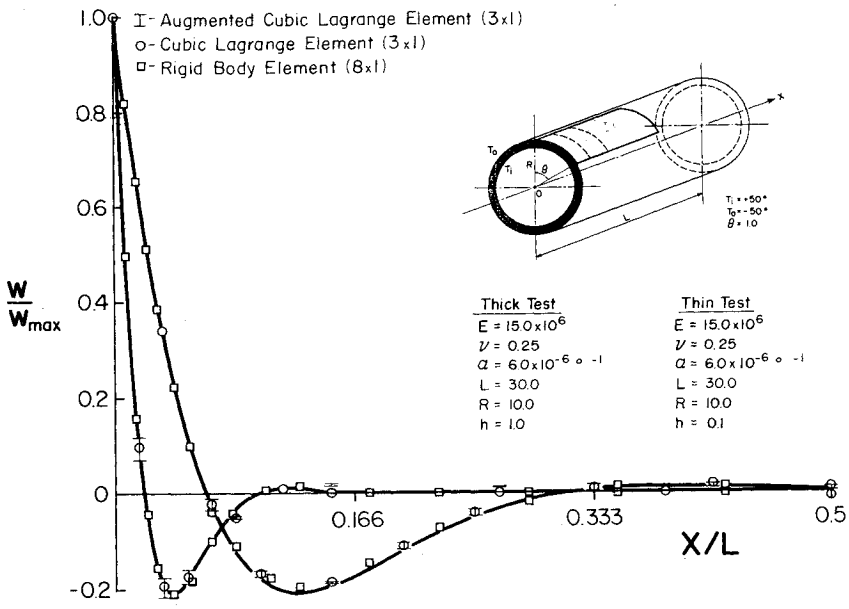

Fig. 5 Thermal test geometries and radial displacement results.

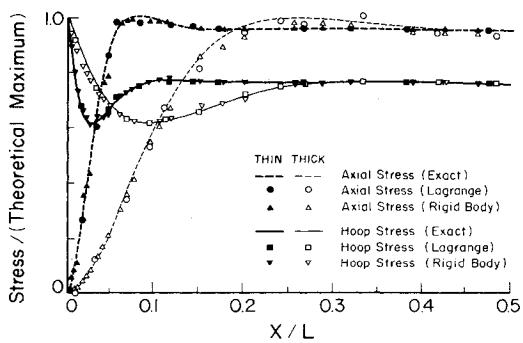

Fig. 6 Stresses at the outer surface for the cylinders with linearly varying temperature through the thickness.

$\Gamma(\theta)$ has a period of 2π and may be uniquely defined if it is known at $(M+1)$ points.

Therefore, it may be represented by a discrete Fourier series of the form

$$\Gamma(\theta) = \frac{1}{2}a_0 + \sum_{j=1}^{k} (a_j \cos j\theta + b_j \sin j\theta) \tag{24}$$

$$a_j = \frac{2}{M+1} \sum_{\alpha=0}^{M} \Gamma(\theta_\alpha) \cos j\theta_\alpha \tag{25}$$

$$b_j = \frac{2}{M+1} \sum_{\alpha=0}^{M} \Gamma(\theta_\alpha) \sin j\theta_\alpha \tag{26}$$

where $\theta_\alpha = 2\pi\alpha/M+1$, $k = \frac{1}{2}M$, and in this case $M=4$.

Upon expanding Eqs. (25) and (26) and substituting the results into Eq. (24) a new form for $\Gamma(\theta)$ may be found which, after collecting coefficients of $\Gamma(\theta_\alpha)$, is expressible as

$$\Gamma(\theta) = \sum_{j=0}^{M} h_j'(\theta)\Gamma(\theta_j), \quad \theta_j = \frac{2\pi j}{M+1} \tag{27}$$

It follows immediately that

$$\int_b^a \Gamma(\theta)\,d\theta = \sum_{j=0}^{M} h_j \Gamma(\theta_j) \tag{28}$$

where

$$h_j = \frac{1}{M+1}\left\{b-a+\sum_{i=1}^{k}\left[\frac{2}{i}\cos(i\theta_j)[\sin(ib)-\sin(ia)]\right.\right.$$
$$\left.\left.-\frac{2}{i}\sin(i\theta_j)[\cos(ib)-\cos(ia)]\right]\right\} \tag{29}$$

Thus, h_j are weighting coefficients which depend only on the interval over which $\Gamma(\theta)$ is integrated and the θ_j are points, not necessarily within the interval of integration, at which Γ must be evaluated. For the developed basis function this integration method is exact and requires little additional computational effort as compared to a Gaussian scheme. Thus, the stiffness matrix may be integrated exactly by a five-point integration scheme in the circumferential direction coupled with a three-point Gaussian scheme in the axial direction. An analogous lower order scheme is readily derivable for the consistent force vector calculations involving distributed line and surface loads where $M=2$ and $k=1$.

Numerical Tests and Results

Five tests were employed to assess the above element. They were the pinch test, an open shell segment roof test, a uniform pressure test on a free-free cylinder, an axisymmetric radially varying temperature distribution, and a prescribed rigid-body translation. The units employed in these examples may be interpreted to be from any self-consistent system of units. Each of these tests shall be discussed in turn and comparisons are made to a cubic Lagrange element based on the same constitutive and strain-displacement relations and a cubic Lagrange element which has been augmented a posteriori in the manner of Cantin[2] to provide the correct rigid-body modes.

A cubic Lagrange element was chosen for comparison purposes because results from other studies suggest it to be a good choice for shell problems[28,34] with regard to its ability to handle rigid-body motions.

The present formulation results in an element with the requisite six zero eigenvalues corresponding to the six rigid-body modes, while the cubic Lagrange element possesses only two zero eigenvalues although its augmented version has the requisite six zero eigenvalues.

Prescribed Translation

For this test a single element encompassing an arc of $\pi/2$ rad was given a prescribed displacement along a single

generator in the direction of the $\theta=0$ radius and the corresponding displacments of the remaining nodes were determined. The results are illustrated in Fig. 3 where only one axial station is shown as there was no axial variation in any of the models.

In these results it is evident that the Lagrange element cannot reproduce the required rigid-body motion in any respect and although the nodal displacements in the augmented Lagrange element are correct the rest of the element has deformed as illustrated. In the case of the rigid-body element, all points are translated correctly making this the only model which is strain-free everywhere, after translation.

Uniform Pressure Test

A uniform normal pressure was applied to a single element of each formulation as illustrated in Fig. 4 with the results shown. Both the Lagrange cubic and the present element produced uniform displacements with negligible error, while the augmented Lagrange element failed to even obtain the correct trend. An analogous result to this is reported by Fonder and Clough[3] for a uniformly pressurized sphere.

Thermal Test

Both thick and thin shell geometries were chosen for this test which consists of a linear temperature distribution through the thickness of the shell, as shown in Fig. 5 where the computed radial displacement is compared to the exact solution,[35] with both the numerical and theoretical results being normalized with respect to the theoretical maximum displacement. For both cases the agreement between the computed and exact solutions is excellent for the Lagrangian element and the present element. Although the results for the augmented element look equally good in Fig. 5 there is a secondary problem, in that the augmented element shows variations in the results in the circumferential direction and hence does not reproduce the axisymmetric nature of the solution.

The computed axial and tangential stresses for the present formulation and the Lagrangian element are compared to the exact values[35] in Fig. 6 where both the numerical and theoretical results are normalized with respect to the theoretical maximum stress in each case. In both shell geometries the tangential stress component is computed to within 2% of the exact solution at all points and the axial stress is computed to within 5%. The lower accuracy achieved in the axial stress case is consistent with the results achieved for Lagrange basis functions and is due to the inability of either type of basis function to match the decaying sinusoidal form of the exact solution adequately. Note that the areas of most rapid change of the displacement or stress gradients do not coincide so that modeling to achieve accuracy in one does not mean accuracy in the others.

Pinch Test

The test geomery along with the test results are illustrated in Fig. 7. For this very demanding test the augmented Lagrange element converges to a value of $\bar{w}=-0.1114$ as do the other two formulations but it is evident that the augmented element converges most rapidly. The difference between this value and the previously obtained value[2] of -0.1139 may result from the present Mindlin vs classical thin shell formulation.

The cubic Lagrange element converges almost as quickly as the augmented version; and the present element, which implicitly possesses the ability to reproduce rigid-body motions, converges most slowly. While this test is very difficult, it would appear from the present results that the difficulty of the problem does not arise so much from the absence or presence of rigid-body mode capability in the element—as advocated in Ref. 34—but from other causes such as large stress or displacement gradients.

Shell Roof Test

A deep, thin shell segment is supported at its two ends by rigid-diaphragm supports, while the longitudinal edges are free to move under the gravitational self weight loading.

This problem has been treated extensively by other authors[36-40] and constitutes a standard test for shell elements. The geometry is given in Fig. 8 along with the results for the axial displacement at the diaphragm and the net vertical displacement around the midspan meridian. The exact solution is due to Scordelis and Lo[36] as reported in Refs. 37 and 38. While the 3×3 mesh of rigid-body elements is outperformed by the 2×2 mesh of Lagrange bicubic elements there is satisfactory convergence illustrated in the refinement to a 4×6 mesh. The results for this finer mesh are superior to those reported in Refs. 37 and 38 for a 4×6 mesh of fully integrated parabolic serendipity elements and are comparable to those reported in Refs. 39 and 40.

The axial stress resultant N_x and the moment resultants M_x and M_y are reported in Fig. 9 where agreement is shown to be very good for N_x and M_x but is less satisfactory for the M_y resultant where the moment resultant value is seen to be almost constant over an element. This phenomenon has its origins in several aspects of the problem. First, the choice of $\nu=0$ has uncoupled the axial strain contribution from the calculation of σ_y so that σ_y depends solely on ϵ_y and, in turn, M_y depends solely on the first-order curvature term in the strain-displacement relation for ϵ_y. Also, since the shell is relatively thin $(R/h=100)$ the rotational degree of freedom ψ_y satisfies the Kirchhoff condition almost exactly. Under

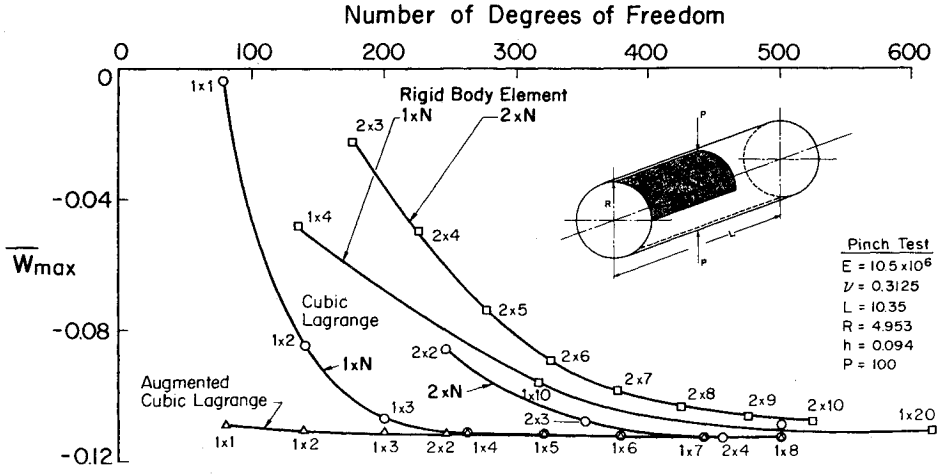

Fig. 7 Pinch test geometry and results.

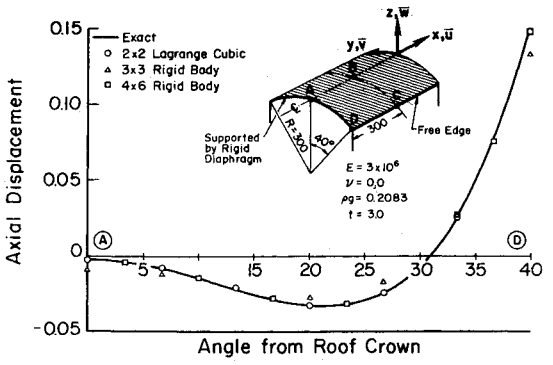

Fig. 8a Shell roof test: Axial displacement at a diaphragm.

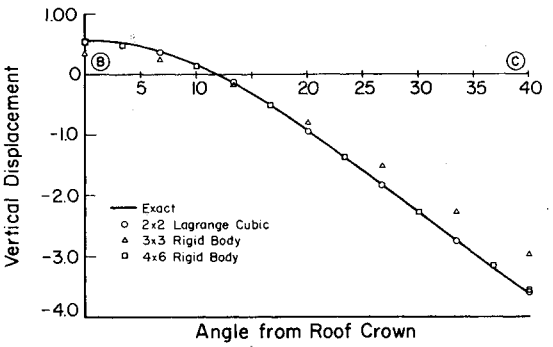

Fig. 8b Shell roof test: Vertical displacement at the midspan.

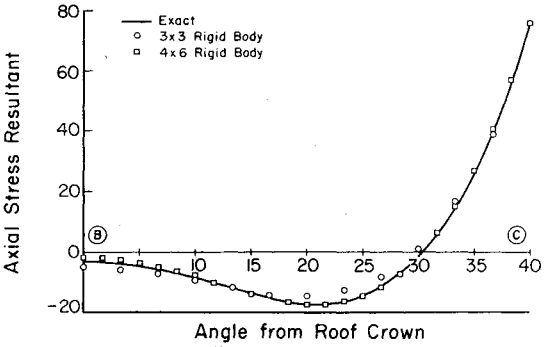

Fig. 9a Shell roof test: Axial stress resultant.

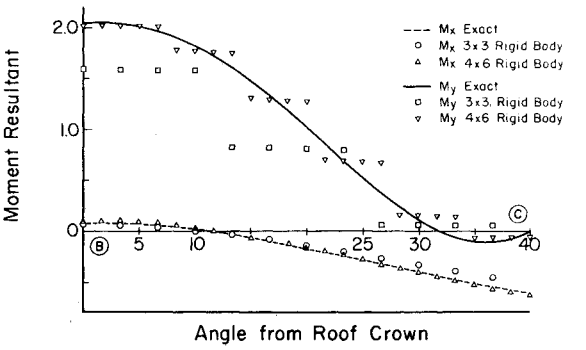

Fig. 9b Shell roof test: Moment resultants.

these circumstances the trigonometric parts of the basis functions can be shown to combine in a manner which allows only a constant value of the first-order curvature term in the strain-displacement relation for ϵ_y, and hence only a constant value for M_y. The degree of constancy exhibited by M_y over an element is a measure of the thinness of the shell. In a thin shell formulation of the same problem using the present basis functions it would be the case that $M_y \equiv$ const.

It may be noted that upon refinement of the mesh, the values of M_y on an element do converge to the correct value and that the problem of $M_y =$ const is also exhibited by fully integrated polynomial trial functions.[38] This relieved by the use of reduced integration techniques which are not acceptable in the present formulation.

Discussion

Of the three formulations investigated, the present element is the only one which gives satisfactory results for each test.

The failure of the Lagrange element to meet the prescribed translation test requirements is not surprising and is directly attributable to the use of polynomial trial functions which cannot reproduce rigid-body motions of this type.

Although the nodal points of the augmented Lagrange element satisfy the prescribed rigid-body motion, other points on the element will not, due to the polynomial trial functions which are employed. Thus there will be nonzero strains present.

The origin of the problems for the augmented Lagrange element in the uniform pressure and the thermal tests is unclear but it may have to do with the following. In the original development of this procedure[2] and its more general form[3] it is required that the product of the applied kinematic transformation T and the applied force vector F be such that $T'^T F \equiv \mathbf{0}$. In the case of the two tests in question, where F is fully populated, this assumption is not satisfied and $T'^T F \neq \mathbf{0}$. In addition, Przemieniecki[41] in a parallel procedure shows that $T'^T F$ does not generally equal zero. Furthermore, the solution for the deformations induced by an axisymmetric load in the augmented Lagrange element is incorrect although it is consistent with that anticipated in the pinch test. This may provide, in part, the reason for this element's success in the pinch test in spite of the above difficulties. Another point of interest is that $T'^T F$ is very nearly zero in the pinch test but this appears to be happenstance.

The present element not only provides accurate displacements but, with one exception as noted above, does equally well in estimating the stresses present in the model. Since this one exception is of explicable origin and there are redeeming convergence characteristics, it is felt that in cases where the satisfaction of rigid-body motion requirements is necessary this is a small shortcoming which should not detract from the use of this element.

Conclusions

The element development herein implicitly possesses the capability to reproduce the six required rigid-body motions, can produce constant strain states, satisfies compatibility requirements by allowing the element degrees of freedom to be continuous across element boundaries, while it displays competitive economy, accuracy, and convergence characteristics.

References

[1] Cantin, G. and Clough, R. W., "A Curved Cylindrical Shell, Finite Element," *AIAA Journal*, Vol. 6, June 1968, pp. 1057-1062.

[2] Cantin, G., "Rigid Body Motions in Curved Finite Elements," *AIAA Journal*, Vol. 8, July 1970, pp. 1252-1255.

[3] Fonder, G. and Clough, R. W., "Explicit Addition of Rigid Body Motions in Curve Finite Elements," *AIAA Journal*, Vol. 11, March 1973, pp. 305-312.

[4] Dawe, D. J., "Rigid Body Motions and Strain-Displacement Equations of Curved Shells Finite Elements," *International Journal of Mechanical Science*, Vol. 14, 1972, pp. 569-578.

[5] Morris, A. J., "A Summary of Appropriate Governing Equations and Functionals in the Finite Element Analysis of Thin Shells," *Finite Elements for Thin Shells and Curved Members*, edited by D. G. Ashwell and R. H. Gallagher, John Wiley & Sons, London, 1976, pp. 15-40.

[6] Cantin, G., "Rigid Body Motions and Equilibrium in Finite Elements," *Finite Elements for Thin Shells and Curved Members*, edited by D. G. Ashwell and R. H. Gallagher, John Wiley & Sons, London, 1976, pp. 55-62.

[7] Fonder, G. A., "Studies in Doubly Curved Elements for Shells of Revolution," *Finite Elements for Thin Shells and Curved Members*, edited by D. G. Ashwell, and R. H. Gallagher, John Wiley & Sons, London, 1976, pp. 113-130.

[8] Gallagher, R. H., "Problems and Progress in Thin Shell Finite Element Analysis," *Finite Elements for Thin Shells and Curved Members*, edited by D. G. Ashwell and R. H. Gallagher, John Wiley & Sons, London, 1976, pp. 1-14.

[9] Irons, B. M., "The Semi Loof Shell Element," *Finite Elements for Thin Shells and Curved Members*, edited by D. G. Ashwell and R. H. Gallagher, John Wiley & Sons, London, 1976, pp. 197-222.

[10] Ashwell, D. G., "Strain Elements with Applications to Arches, Rings and Cylindrical Shells," *Finite Elements for Thin Shells snd Curved Members*, edited by D. G. and Ashwell, R. H. Gallagher, John Wiley & Sons, London, 1976.

[11] Nanyaro, A. P., "A Study of Crashworthiness of Light Aircraft Fuselage Structures: A Numerical and Experimental Investigation," Ph.D. Thesis, Institute for Aerospace Studies, University of Toronto, Canada, 1983.

[12] Tennyson, R. C., Teichman, H., Nanyaro, A. P., and Mabson, G., "Study of Crashworthiness of Light Fuselage Structures," AIAA Paper 81-0574, *Proceedings of the ASCE/AIAA/ASME/AHS 22nd Structures, Structural Dynamics and Materials Conference*, April 1981.

[13] Nanyaro, A. P., "Crash Dynamic Analysis of Light Aircraft Structures Using Finite Element Formulation," Paper 2-2, 1st Canadian Symposium on Aerospace Structures and Materials, Toronto, Canada, June 1982.

[14] Mindlin, R. D., "Influence of Rotary Inertia and Shear on Flexural Motions of Elastic Plates," *Journal of Applied Mechanics*, Vol. 18, March 1951, pp. 31-38.

[15] Ahmad, S., Irons, B. M., and Zienkiewicz, O. C., "Analysis of Thick and Thin Shell Structures by Curved Finite Elements," *International Journal for Numerical Methods in Engineering*, Vol. 2, 1970, pp. 419-451.

[16] Zienkiewicz, O. C., Taylor, R. L., and Too, J. M., "Reduced Integration Technique in General Analysis of Plates and Shells," *International Journal for Numerical Methods in Engineering*, Vol. 3, April-June 1971, pp. 275-290.

[17] Zienkiewicz, O. C. and Hinton, E., "Reduced Integration Function Smoothing and Non-Conformity in Finite Element Analysis (with Special Reference to Thick Plates)," *Journal of the Franklin Institute*, Vol. 302, Nov./Dec. 1976, pp. 443-461.

[18] Noor, A. K. and Mathers, M. D., "Finite Element Analysis of Anisotropic Plates," *International Journal for Numerical Methods in Engineering*, Vol. 11, No. 2, 1977, pp. 289-307.

[19] Onate, E., Hinton, E., and Glover, N., "Techniques for Improving the Ahmad Shell Element," *International Conference on Applied and Numerical Modelling*, Madrid, 1978, pp. 389-399.

[20] Pugh, E. D. L., Hinton, E., and Zienkiewic, O. C., "A Study of Quadrilateral Plate Bending Elements with Reduced Integration," *International Journal for Numerical Methods in Engineering*, Vol. 12, July 1978, pp. 1059-1079.

[21] Hughs, T.J.R. and Cohen, M., "The Heterosis Finite Element for Plate Bending," *Computers and Structures*, Vol. 9, Nov. 1978, pp. 445-450.

[22] McNeill, N. J., "An Improved Mindlin Plate Bending Element and the Compatible Quarter Point Crack Tip Derivative," M.A.Sc. Thesis, Dept. of Aerospace Science and Engineering, University of Toronto, Canada, 1982.

[23] Reissner, E., "The Effect of Transverse Shear Deformation on the Bending of Elastic Plates," *Journal of Applied Mechanics, Transactions of ASME*, June 1945, pp. A69-A77.

[24] Goodier, J. N., Discussion of Ref. 23, "The Effect of Transverse Shear Deformation on the Bending of Elastic Plates," *Journal of Applied Mechanics, Transactions of ASME*, Vol. 68, Sept. 1946, pp. A249-A252.

[25] Reissner, E., "On Bending of Elastic Plates," *Quarterly of Applied Mathematics*, Vol. 5, No. 1, 1947, pp. 55-68.

[26] Green, A. E., "On Reissner's Theory of Bending of Elastic Plates," *Quarterly of Applied Mathematics*, Vol. 7, No. 2, 1949, pp. 223-228.

[27] Vlasov, V. S., "Basic Differential Equations in General Theory of Elastic Shells," NACA TM-1241, 1951.

[28] Ashwell, D. G. and Gallagher, R. H., *Finite Elements for Thin Shells and Curved Members*, John Wiley & Sons, London, 1976.

[29] Laanghaar, H. L., *Energy Methods in Applied Mechanics*, John Wiley & Sons, New York, 1962.

[30] Vlasov, V. Z., "General Theory of Shells and Its Applications to Engineering," Translation, NASA TT F-99, April 1964.

[31] Heppler, G. R. and Hansen, J. S., "A Mindlin Element for Thick Deep Shells," to be published.

[32] Strang, G. and Fix, G., *Analysis of the Finite Element Method*, Prentice-Hall, Englewood Cliffs, N. J., 1973.

[33] Dahlquist, G. and Bjorck, A., *Numerical Methods*, translated by Ned Anderson, Prentice-Hall, Englewood Cliffs, N.J., 1974.

[34] Thomas, G. R. and Gallaher, R. H., "A Triangular Element Based on Generalized Potential Energy Concepts," *Finite Elements for Thin Shells and Curved Members*, edited by D. G. Ashwell and R. H. Gallagher, John Wiley & Sons, London, 1976, pp. 155-169.

[35] Kent, C. H., "Thermal Stresss in Thin Walled Cylinders," *Transactions of ASME*, Vol. 53, 1931, pp. 167-180.

[36] Scordelis, A. C. and Lo, K. S., "Computer Analysis of Cylindrical Shells," *American Concrete Institute Journal*, Vol. 61, May 1964, pp. 539-560.

[37] Ahmad, S., Irons, B. M., and Zienkiewicz, O. C., "Analysis of Thick and Thin Shell Structues by Curved Finite Elements," *International Journal for Numerical Methods in Engineering*, Vol. 2, 1970, pp. 419-451.

[38] Zienkiewicz, O. D., Taylor, R. L., and Too, J. M., "Reduced Integration Technique in General Analysis of Plates and Shells," *International Journal for Numerical Methods in Engineering*, Vol. 3, April-June 1971, pp. 275-290.

[39] Kiciman, O. K., and Popov, E. P., "A General Finite Element Model for Shells of Arbitrary Geometry," *Computational Methods in Applied Mechanical Engineering*, Vol. 13, Jan. 1978, pp. 45-58.

[40] Sander, G. and Idelsohn, S., "A Family of Conforming Finite Elements for Deep Shell Analysis," *International Journal of Numerical Methods in Engineering*, Vol. 18, March 1982, pp. 363-380.

[41] Przemieniecki, J. S., *Theory of Matrix Structural Analysis*, McGraw-Hill Book Co., New York, 1968.